Anesthesiology 2005; 103:306–17

Quantifying Mechanical Heterogeneity in Canine Acute Lung Injury

Impact of Mean Airway Pressure

David W. Kaczka, M.D., Ph.D., David N. Hager, M.D.,† Monica L. Hawley, Ph.D.,‡ Brett A. Simon, M.D., Ph.D.§*

Background: **The heterogeneous pattern of acute lung injury (ALI) predisposes patients to ventilator-associated lung injury. Currently, there is no simple technique that can reliably quantify lung heterogeneity during the dynamic conditions of mechanical ventilation. Such a technique may be of use in optimizing mechanical ventilatory parameters such as rate, tidal volume, or positive end-expiratory pressure.**

Methods: **To determine the impact of heterogeneity on respiratory mechanics, the authors measured respiratory impedance (Z_{rs}), expressed as respiratory resistance (R_{rs}) and elastance (E_{rs}), in 11 anesthetized dogs from 0.078 to 8.9 Hz using broadband pressure and flow excitations under baseline conditions and after ALI produced by infusion of 0.08 ml/kg oleic acid into the right atrium. Data were obtained at mean airway pressures ($\bar{P}_{ao}$) of 5, 10, 15, and 20 cm H_2O. The Z_{rs} spectra were fit by various models of the respiratory system incorporating different distributions of parallel viscoelastic tissue properties.**

Results: **Under baseline conditions, both R_{rs} and E_{rs} exhibited dependence on oscillation frequency, reflecting viscoelastic behavior. The E_{rs} demonstrated significant dependence on $\bar{P}_{ao}$. After ALI, both the level and frequency dependence of R_{rs} and E_{rs} increased, as well as the apparent heterogeneity of tissue properties. Both R_{rs} and E_{rs} as well as heterogeneity decreased with increasing $\bar{P}_{ao}$, approaching baseline levels at the highest levels of $\bar{P}_{ao}$.**

Conclusions: **These data demonstrate that Z_{rs} can provide specific information regarding the mechanical heterogeneity of injured lungs at different levels of $\bar{P}_{ao}$. Moderate increases in $\bar{P}_{ao}$ seem to be beneficial in ALI by reducing heterogeneity and recruiting lung units. These noninvasive measurements of lung heterogeneity may ultimately allow for the development of better ventilation protocols that optimize regional lung mechanics in patients with ALI.**

ACUTE lung injury (ALI) is a complex pathologic process involving a heterogeneous interaction of mechanical and biochemical processes.[1] Although there are many etiologies for this syndrome, it is ultimately characterized by respiratory failure in the presence of airway closure and atelectasis, alveolar flooding, increased lung resistance, reduced lung compliance, and impairments in gas exchange.[1,2] The current mainstay of treatment is supportive therapy with tracheal intubation and mechanical ventilation.[1] Given the heterogeneous nature of this disease, positive-pressure ventilation may expose certain regions of the lung to further injury due to either an unequal distribution of inspired volume, resulting in high alveolar pressures and overdistention, or repetitive end-expiratory derecruitment and reopening.[3,4] Because such ventilator-associated lung injury is the direct result of the heterogeneous nature of the injury, the ability to quantify mechanical heterogeneity may be useful in optimizing ventilatory parameters such as positive end-expiratory pressure (PEEP), tidal volume, or frequency.

The forced oscillation method to measure respiratory input impedance (Z_{rs}), the complex ratio of pressure to flow at the airway opening as a function of frequency, is gaining increasing acceptance as a valid method for assessing dynamic mechanical properties of the respiratory system.[5] When measured over frequencies ranging from approximately 0.1 to 10.0 Hz, Z_{rs} is a sensitive indicator of serial and parallel airway heterogeneity,[6–8] provides insight into the locus of airway obstruction in asthma and chronic obstructive pulmonary disease,[9,10] and may be useful in partitioning the mechanical properties of the lung tissues.[11]

The goal of this study was to characterize the dynamic mechanical behavior of the respiratory system in a canine model of ALI. We used the frequency-dependent features of Z_{rs}, specifically respiratory resistance (R_{rs}) and elastance (E_{rs}), to assess the degree and severity of lung injury in dogs after administration of oleic acid. Particular emphasis was placed on quantifying mechanical heterogeneity before and after injury at different levels of mean airway pressure ($\bar{P}_{ao}$). The motivation for this work arises from recent morphometric modeling studies that demonstrate a strong association between the heterogeneity of airway constriction and the frequency-dependent features of R_{rs} and E_{rs}.[6,8,12–14] Although the structure–function relation of the respiratory system is extremely complex, we reasoned that the heterogeneous changes in regional lung elastances occurring in ALI may affect Z_{rs} in a specific and predictable manner. Furthermore, we hypothesized that as $\bar{P}_{ao}$ increased and lung regions became more uniformly ex-

* Assistant Professor of Anesthesiology and Critical Care Medicine and Biomedical Engineering, † Fellow in Pulmonary and Critical Care Medicine, § Associate Professor of Anesthesiology and Critical Care Medicine, The Johns Hopkins University School of Medicine, Baltimore, Maryland. ‡ Adjunct Assistant Professor of Otolaryngology, University of Maryland School of Medicine, Baltimore, Maryland.

Received from the Departments of Anesthesiology and Critical Care Medicine and Biomedical Engineering, The Johns Hopkins University, Baltimore, Maryland. Submitted for publication December 20, 2004. Accepted for publication April 6, 2005. Supported by a Research Starter Grant from the Foundation for Anesthesia Education and Research, Rochester, Minnesota, and grant No. R01 HL-58504 from the National Institutes of Health, Washington, D.C. Dr. Kaczka is listed as primary inventor on a provisional U.S. Patent for the pneumatic oscillator described in the Materials and Methods section of the manuscript, which is owned by the Trustees of Boston, University, Boston, Massachusetts. Currently, there are no licensing agreements between Dr. Kaczka and Boston University or any other third party regarding this technology.

Address reprint requests to Dr. Kaczka: Department of Anesthesiology and Critical Care Medicine, The Johns Hopkins Hospital, 600 North Wolfe Street, Meyer 299C, Baltimore, Maryland 21287. Address electronic mail to: dkaczka1@jhmi.edu. Individual article reprints may be purchased through the Journal Web site, www.anesthesiology.org.

panded, there would be characteristic changes in Z_{rs}, reflecting the process of recruitment and possibly a reduction in lung heterogeneity.

The specific aims of this study were (1) to measure Z_{rs} in mongrel dogs at baseline and after ALI induced with oleic acid; (2) to use an inverse distributed modeling approach to characterize Z_{rs} in terms of different distributions of respiratory tissue heterogeneity; and (3) to investigate the impact of $\bar{P}_{ao}$ on Z_{rs} and by extension, on mechanical heterogeneity.

Materials and Methods

Animal Preparation and Measurements

Measurements were made in 11 mongrel dogs weighing between 7.6 and 20.0 kg. The protocol was approved by the Johns Hopkins Animal Care and Use Committee (Baltimore, Maryland) to ensure humane treatment of animals. Each dog was anesthetized with pentobarbital given intravenously (25 mg/kg at induction with 5 mg/kg hourly maintenance), relaxed with pancuronium, orally intubated with an 8.0-mm-ID endotracheal tube, and mechanically ventilated (initial rate 20 min^{-1} and tidal volume 15 ml/kg, titrated to achieve an end-tidal level between 30 and 40 mmHg, and 5 cm H_2O PEEP). Oxygen saturation was continuously monitored with a pulse oximeter applied to the tongue. Femoral arterial and venous catheters were inserted *via* femoral cut-down, and a pulmonary artery catheter (7.5 French; Edwards Lifesciences LLC, Irvine, CA) was inserted through the femoral vein. Systemic arterial, pulmonary arterial, and central venous pressures were continuously monitored (Tram-Rac 4A; GE Marquette Medical Systems, Milwaukee, WI). Cardiac output was measured in triplicate using the thermodilution technique. Airway flow was measured with a pneumotachograph (Hans Rudolph 4700A; Kansas City, MO) coupled to a pressure transducer (Honeywell DC001NDC4 $\pm$ 1 in H_2O; Morristown, NJ). Tracheal pressure was measured with an additional pressure transducer (Honeywell DC020NDC4 $\pm$ 20 in H_2O) attached to a small polyethylene catheter placed through the endotracheal tube and allowed to extend approximately 2 cm into the trachea.[15] An intravenous infusion of lactated Ringer's (15 ml $\cdot$ kg^{-1} $\cdot$ h^{-1}) was given for maintenance fluid replacement.

Protocol

To measure Z_{rs} , each dog was disconnected from the conventional mechanical ventilator and connected to a custom-built servo-controlled pneumatic pressure oscillator.[16] This device is based on a proportional solenoid valve (ASCO Posiflow model SD8202G4V; Florham Park, NJ) that adjusts flow in proportion to an applied voltage and is incorporated into a closed-loop arrangement that provides accurate control of $\bar{P}_{ao}$ during superimposed oscillations. To standardize volume history, a deep inflation to 30 cm H_2O was first performed, and then tracheal pressure was reduced to a specified $\bar{P}_{ao}$. A discretized broadband pressure excitation signal with energy between 0.078 to 8.9 Hz was generated at a sampling rate of 40 Hz using a digital-to-analog converter (Data Translations DT-2811; Marlboro, MA). This digital signal consisted of nine sinusoids with equivalent amplitudes and random phases, with frequency components chosen to obey a nonsum nondifference criterion to minimize the impact of nonlinearities in computations of Z_{rs}.[17] The digital signal was low-pass filtered at 10 Hz (Frequency Devices 858L8B-2; Haverhill, MA) and presented to the electronic control unit of the proportional solenoid. The net amplitude of the driving signal was adjusted to yield a delivered tidal volume of approximately 50 ml root mean square, as computed using trapezoidal integration of the sampled flow waveform. Corresponding tracheal pressure and flow signals were low-pass filtered at 10 Hz and sampled at 40 Hz by an analog-to-digital converter (Data Translations DT-2811) for subsequent processing. Between oscillatory pressure excitations, the dog was reconnected to the ventilator for a period of 4–5 min. The Z_{rs} measurements were obtained at $\bar{P}_{ao}$ levels of 5, 10, 15, and 20 cm H_2O applied in random order.

Lung injury was then induced by infusing 0.08 ml/kg oleic acid (Sigma-Aldrich, Inc., St. Louis, MO) into the right atrial port of the pulmonary artery catheter over 20 min. After allowing 90–120 min for the injury to stabilize, clinical signs of severe pulmonary injury were evident, including bilateral crackles and wheezes, and oxygen saturation less than 91% with inspired oxygen fraction equal to 1.0. The Z_{rs} measurements were then repeated as above. Dogs were killed with an intravenous overdose of pentobarbital (10–20 mg/kg) followed by rapid injection of 50 ml saturated solution of potassium chloride.

Signal Processing

Respiratory impedance Z_{rs} and its coherence function γ^2 were determined using an overlap-average periodogram technique.[18] Each Z_{rs} spectrum was computed using a 25.6-s time window with 83% overlap. After neglecting the first 1,000 points in the data record (approximately 25 s) to minimize the influence of transient responses, between 12 and 20 overlapping windows were used to calculate Z_{rs} for each animal. Total R_{rs} was determined as the real part of Z_{rs} only at those frequencies f_k where input energy was placed: $R_{rs}(f_k) = \mathrm{Re}\{Z_{rs}(f_k)\}$. The effective E_{rs} was calculated from the imaginary part: $E_{rs}(f_k) = -2\pi f_k \, \mathrm{Im}\{Z_{rs}(f_k)\}$. In no instance did we find that γ^2 was less than 0.95 at any f_k.

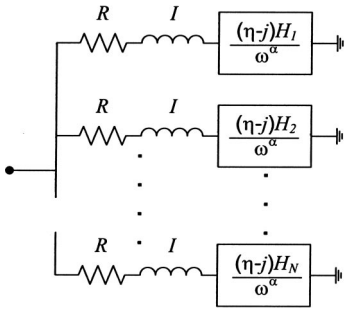

Fig. 1. Model of the respiratory system with a parallel arrangement of *N* branches, each consisting of equivalent linear resistance (*R*) and inertance (*I*) elements and subtended by a viscoelastic tissue element. The tissue elements have equivalent hysteresivity parameters (η) but distinct tissue elastance parameters ($H_1, H_2, \ldots, H_N$) that may vary from branch to branch in a probabilistic manner. The exponent α depends on η: $\alpha = (2/\pi)\tan^{-1}(1/\eta)$; ω: angular frequency; and j: unit imaginary number (*i.e.*, $\sqrt{-1}$).

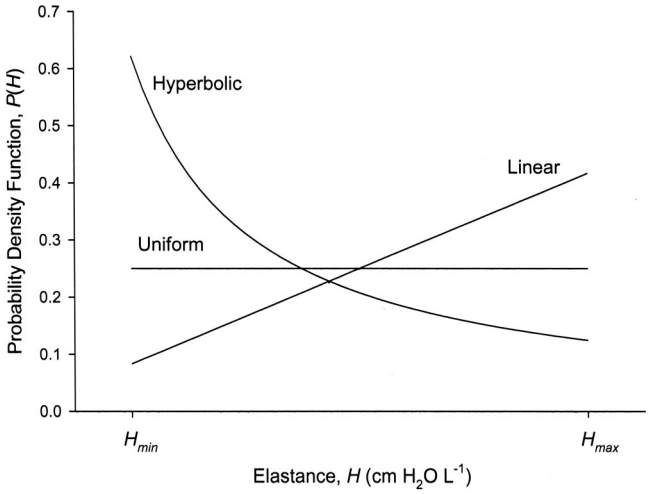

Fig. 2. Continuous probability density functions used for describing tissue heterogeneity with upper and lower tissue elastance bounds H_{min} and H_{max}, respectively.

Modeling Analysis

To interpret the Z_{rs} spectra and quantify parallel tissue heterogeneity, we modified the distributed modeling approach of Suki and coworkers.[19–22] We modeled the respiratory system as a parallel arrangement of branches with equivalent linear resistive (*R*) and inertial (*I*) elements, with each branch subtended by a unique viscoelastic constant-phase tissue element (fig. 1).[23] These branches do not represent distinct anatomical structures, but rather discrete functional compartments that uniquely contribute to the overall mechanical properties of the respiratory system. The *R* element is a frequency-independent parameter reflecting both airway resistance as well as the purely Newtonian component of chest wall resistance.[24] The *I* element accounts primarily for the inertia of gas in the central airways with a small contribution from the mass of the parenchymal tissues and chest wall. The viscoelastic tissue elements are characterized by identical hysteresivity parameters (η), which account for the dynamic pressure–volume hysteresis of the respiratory tissues (*i.e.*, tissue resistance), but unique elastance parameters ($H_1, H_2, \ldots, H_N$) that vary from branch to branch according to a continuous probability density function *P*(*H*). Therefore, the distribution of tissue elements allow for frequency dependence in R_{rs} and E_{rs} by two distinct mechanisms: viscoelasticity[11,23] and parallel heterogeneity.[6,8,25]

To obtain closed-form expressions for the model-predicted impedance (appendix), we assumed *P*(*H*) followed either hyperbolic, linear, or uniform distributions defined over minimum (H_{min}) and maximum (H_{max}) values (fig. 2). The uniform distribution does not imply a homogeneous lung; rather, it assumes that the estimated distribution of tissue elastances ranging from H_{min} to H_{max} occur with equal probability. Regardless of the form of the distribution function, the model consisted of five independent parameters (R, I, η, H_{min}, and H_{max}), which were estimated using a nonlinear gradient technique that minimized the sum of squared differences between actual Z_{rs} spectrum and the corresponding model prediction (Matlab version 7.0; The Mathworks, Natick, MA). If the gradient search algorithm converged to a unique solution for two or more model distributions, the most appropriate distribution for a given Z_{rs} spectrum was established using the corrected Akaike Information Criterion (AIC_C).[26,27] For the model with the lowest AIC_C score, we determined its relative likelihood of being the best model among the other candidates using the technique of Akaike weights.[28] Based on the mean and SD of this selected distribution function, we computed an effective tissue elastance (μ_H) and heterogeneity index (σ_H) for each Z_{rs}.

Statistical Analysis

To assess the impact of $\bar{P}_{ao}$ and injury on the overall levels of impedance, we computed the average magnitude of Z_{rs} across all frequencies:

$$|\bar{Z}_{rs}| = \frac{1}{K}\sum_{k=1}^{K}\sqrt{(\mathrm{Re}\{Z_{rs}(f_k)\})^2 + (\mathrm{Im}\{Z_{rs}(f_k)\})^2},$$

where K is the total number of frequencies in the pressure excitation signal. A one-way analysis of variance (ANOVA) of the four $\bar{P}_{ao}$ levels (5, 10, 15, and 20 cm H_2O) was used to compare values of R_{rs} and E_{rs} at each f_k, $|\bar{Z}_{rs}|$, the five model parameters from the most appropriate distribution function, as well as μ_H, and σ_H before and after injury (SAS version 8.2; SAS Institute Inc., Cary, NC). If significance was obtained with ANOVA, *post hoc* analysis was performed using the least significant difference criterion. At each $\bar{P}_{ao}$, preinjury and postinjury

Table 1. Gas Exchange and Hemodynamic Data for the 11 Dogs at Baseline and after ALI

	Baseline	After Injury
HR, beats/min	133 ± 25	108 ± 20*
CO, l/min	3.02 ± 0.83	1.72 ± 0.63§
MSAP, mmHg	111 ± 16	100 ± 20
MPAP, mmHg	17 ± 4	23 ± 7†
RR, breaths/min	20 ± 3	19 ± 3
V_T, ml	236 ± 53	268 ± 69*
pH	7.34 ± 0.06	7.26 ± 0.07
$Paco_2$, mmHg	38.6 ± 6.6	42.1 ± 6.2
Pao_2/Fio_2, mmHg	528 ± 77	261 ± 125‡
$\dot{Q}_S/\dot{Q}_T$	0.14 ± 0.09	0.32 ± 0.12†
Hemoglobin, g/dl	9.4 ± 1.3	10.5 ± 1.5*

* $P < 0.05$, † $P < 0.01$, ‡ $P < 0.001$, § $P < 0.0001$ *vs.* baseline.

ALI = acute lung injury; CO = cardiac output; Fio_2 = fraction of inspired oxygen; HR = heart rate; MPAP = mean pulmonary arterial pressure; MSAP = mean systemic arterial pressure; $Paco_2$ = arterial partial pressure of carbon dioxide; Pao_2 = arterial partial pressure of oxygen; $\dot{Q}_S/\dot{Q}_T$ = shunt fraction; RR = respiratory rate; V_T = tidal volume.

comparisons of all variables were made using two-tailed paired *t* tests. $P < 0.05$ was considered statistically significant.

Results

Hemodynamic and Gas Exchange Data

Baseline and postinjury hemodynamic and gas exchange data during conventional mechanical ventilation are shown in table 1. After lung injury, we observed significant decreases in heart rate, cardiac output, and the arterial partial pressure of oxygen/fraction of inspired oxygen ratio and significant increases in mean pulmonary arterial pressure, shunt fraction, and hemoglobin concentration.

Impedance Data

Figure 3 shows examples of R_{rs} and E_{rs} spectra in two representative dogs measured at baseline and after lung injury at $\bar{P}_{ao}$ levels of 5, 10, 15, and 20 cm H_2O. Also shown are the corresponding fits to the data from the model of figure 1 using the most appropriate distribution function $P(H)$ based on the minimum AIC_C score. For dog A, which exhibited a relatively minor response to oleic acid based on the degree of changes in Z_{rs}, a model comprising a linear distribution of tissue elastances was sufficient to describe the Z_{rs} spectra at nearly all $\bar{P}_{ao}$ values. Dog B was considered a more severe responder to oleic acid, with baseline Z_{rs} at most values of $\bar{P}_{ao}$ best described by a linear distribution of elastances but postinjury Z_{rs} better characterized by a uniform distribution. For both dogs, baseline levels of E_{rs} increased with increasing $\bar{P}_{ao}$, regardless of frequency.

Figure 4 shows a summary of the R_{rs} and E_{rs} spectra for all 11 dogs at baseline and after ALI at the four levels of $\bar{P}_{ao}$. At baseline, R_{rs} demonstrated a frequency-dependent decrease throughout the bandwidth under excitation for all values of $\bar{P}_{ao}$. The E_{rs} demonstrated a slight positive frequency dependence up to approximately 2 Hz, beyond which it demonstrated a frequency-dependent decrease and often became negative at the highest frequencies. This high frequency decrease results from the effect of gas inertia in the central airways on the

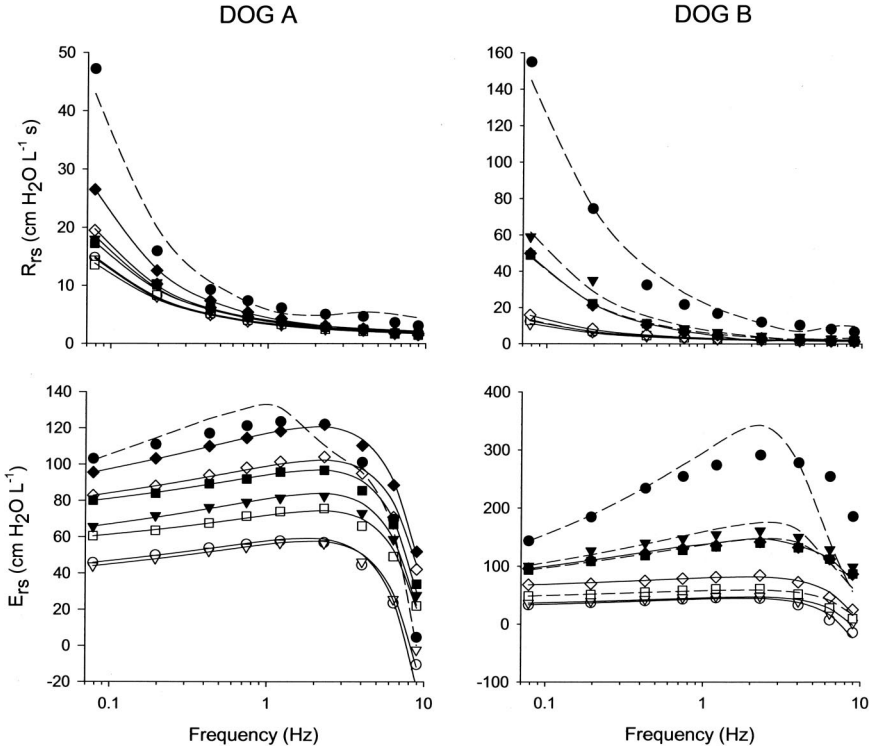

Fig. 3. Examples of respiratory resistance (R_{rs}) and elastance (E_{rs}) *versus* frequency in two representative dogs measured at baseline (*open symbols*) and after lung injury (*closed symbols*). Data were obtained at mean airway pressure ($\bar{P}_{ao}$) levels of 5 (*circles*), 10 (*inverted triangles*), 15 (*squares*), and 20 (*diamonds*) cm H_2O. Shown also are model fits from the most appropriate distribution for a particular Z_{rs}, for these dogs either linear (*solid line*) or uniform (*dashed line*) distributions. Note differences in vertical axes scales between the two dogs.

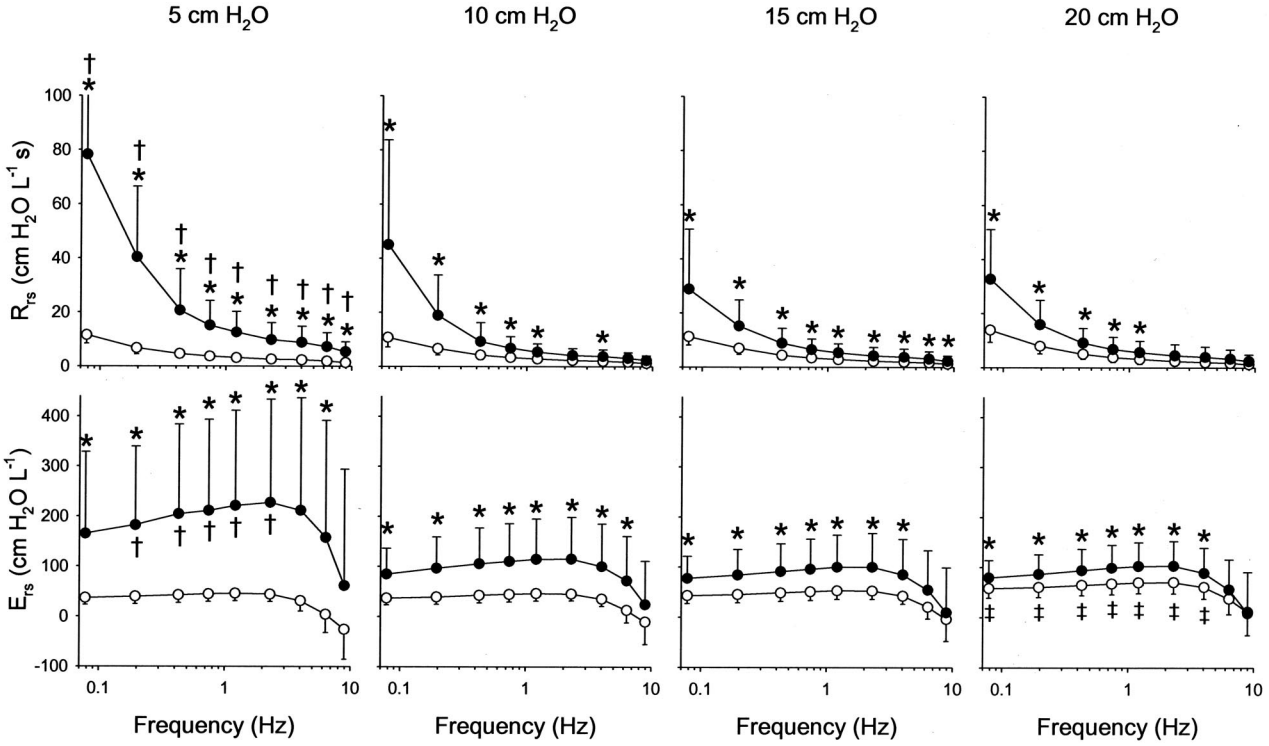

Fig. 4. Summary of respiratory resistance (R_{rs}) and elastance (E_{rs}) from 0.078 to 8.9 Hz at baseline (○) and after oleic acid injury (●) at four different mean airway pressures ($\bar{P}_{ao}$) for all 11 dogs. Values are presented as mean ± SD. Significantly higher from baseline data at same frequency and $\bar{P}_{ao}$ using two-tailed paired *t* test. † Significantly higher than corresponding data at 10, 15, and 20 cm H_2O at same condition and frequency using analysis of variance and least significant difference criterion. ‡ Significantly higher from corresponding data at 5, 10, and 15 cm H_2O at same condition and frequency using analysis of variance and least significant difference criterion.

respiratory system reactance, from which the E_{rs} spectrum is computed. At baseline, the E_{rs} at 20 cm H_2O was significantly higher over the 0.07- to 4.02-Hz range compared with 5, 10, and 15 cm H_2O. After lung injury, both R_{rs} and E_{rs} exhibited increases in their respective mean levels and dependence on frequency compared with baseline for all values of $\bar{P}_{ao}$. Significant increases in R_{rs} and E_{rs} after ALI were observed using paired *t* tests at each f_k as shown in figure 4. After ALI, R_{rs} at 5 cm H_2O $\bar{P}_{ao}$ was significantly higher compared with 10, 15, and 20 cm H_2O $\bar{P}_{ao}$ at all frequencies, although the E_{rs} at 5 cm H_2O was higher only for frequencies between 0.20 and 2.31 Hz.

The impact of injury and $\bar{P}_{ao}$ on $|\bar{Z}_{rs}|$ is shown in figure 5. At baseline, $|\bar{Z}_{rs}|$ at 20 cm H_2O was significantly higher compared with 5, 10, and 15 cm H_2O. After lung injury, significant increases in $|\bar{Z}_{rs}|$ were observed at all values of $\bar{P}_{ao}$ and $|\bar{Z}_{rs}|$ was significantly increased at $\bar{P}_{ao}$ = 5 cm H_2O compared with all other values of $\bar{P}_{ao}$.

Model Analysis

Figure 6 shows a summary of the most appropriate distribution functions as selected according to AIC_C score for all 11 dogs at each $\bar{P}_{ao}$ at baseline and after lung injury. At baseline, the Z_{rs} for most dogs was best described by a linear distribution of tissue elastances. After lung injury, there was an increase in the number of dogs for which Z_{rs} was best described by a uniform distribution of tissue elastances, although the majority of dogs were still best characterized by a linear distribution. A summary of the Akaike weights for the selected model

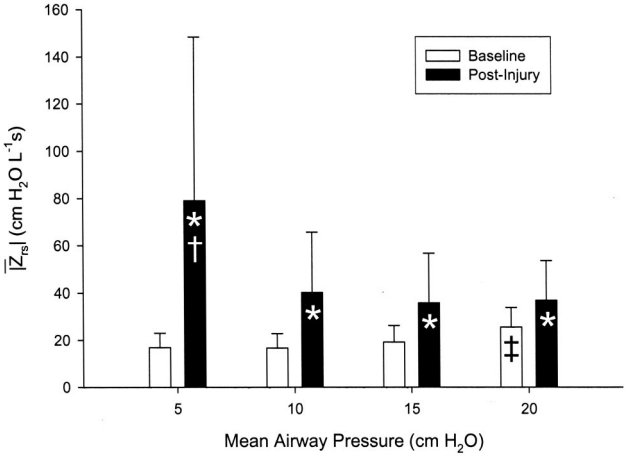

Fig. 5. Summary of average impedance magnitude $|\bar{Z}_{rs}|$ at baseline (*white*) and after oleic acid injury (*black*) at four different mean airway pressures ($\bar{P}_{ao}$) for all 11 dogs. Values are presented as mean ± SD. * Significantly higher from baseline data using two-tailed paired *t* test. † Significantly higher than corresponding data at 10, 15, and 20 cm H_2O at same condition using analysis of variance and least significant difference criterion. ‡ Significantly higher from corresponding data at 5, 10, and 15 cm H_2O at same condition using analysis of variance and least significant difference criterion.

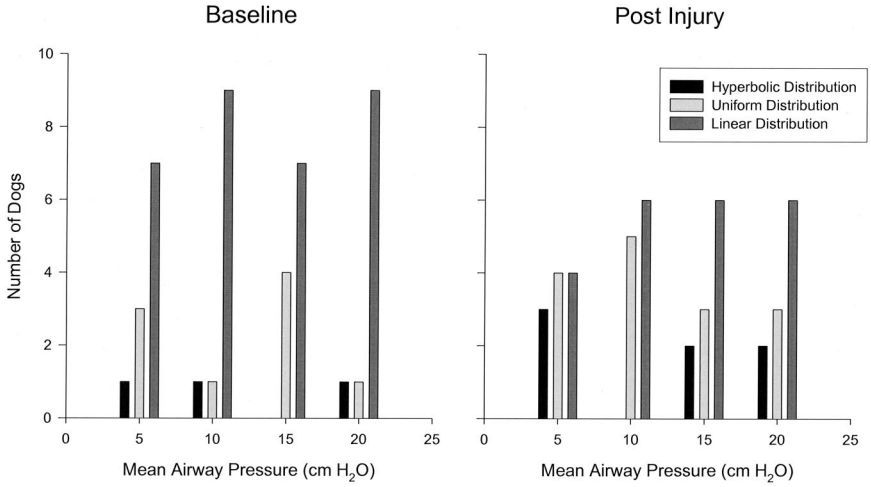

Fig. 6. Summary of tissue elastance distributions obtained for all 11 dogs at baseline and after lung injury at four different values of mean airway pressure ($\bar{P}_{ao}$). At baseline, the Z_{rs} obtained in most dogs was best described by a model incorporating a linear distribution of tissue elastances, regardless of $\bar{P}_{ao}$. After injury, the number of dogs requiring a model with a uniform distribution of tissue elastances increased for 5, 10, and 20 cm H_2O.

distributions is shown in table 2, along with the number of dogs for which two or more model distributions converged for a particular Z_{rs} data set using the nonlinear gradient search algorithm. Under baseline conditions, the likelihoods that the selected distribution generated the data when compared to the alternate candidate distributions ranged from 85.4 to 90.5% as averaged at each $\bar{P}_{ao}$. After lung injury, the likelihoods decreased at all values of $\bar{P}_{ao}$, with mean values ranging from 60.2 to 77.8%. No clear trend of Akaike weight on $\bar{P}_{ao}$ was observed. Although at least one distribution function converged for every Z_{rs} data set examined, the number of dogs for which two or more distribution functions converged decreased after lung injury.

A summary of the estimated model parameters is shown in figure 7. The R parameter, reflecting both airway resistance and the Newtonian component of chest wall resistance, demonstrated no significant dependence on $\bar{P}_{ao}$ during baseline or ALI conditions. Although R demonstrated considerable intersubject variability after lung injury, there was no significant difference between preinjury and postinjury R at any $\bar{P}_{ao}$. The I parameter, reflecting the total inertia of the respiratory system, exhibited no significant dependence on $\bar{P}_{ao}$ at baseline. After lung injury, I significantly increased compared with baseline at all $\bar{P}_{ao}$ values. ANOVA demonstrated a significant dependence of postinjury estimates of I on $\bar{P}_{ao}$, with its value at 5 cm H_2O significantly higher compared with 15 and 20 cm H_2O. Baseline values of the hysteresivity parameter η were within the range reported by previous studies[9,11,29] and significantly increased after lung injury at all $\bar{P}_{ao}$ levels. Neither the H_{min} nor the H_{max} parameters demonstrated any dependence on $\bar{P}_{ao}$ at baseline. ANOVA demonstrated a significant dependence of H_{max} on $\bar{P}_{ao}$ after lung injury, with its value at 5 cm H_2O significantly higher than that at 10, 15, or 20 cm H_2O. After injury, H_{min} increased significantly only at 20 cm H_2O, whereas H_{max} increased significantly at 5, 10, and 15 cm H_2O.

Figure 8 shows the impact of $\bar{P}_{ao}$ and injury on the derived effective tissue elastance (μ_H) and heterogeneity index (σ_H). At baseline, ANOVA demonstrated no significant dependence of either μ_H or σ_H on $\bar{P}_{ao}$. After ALI, μ_H significantly increased at all $\bar{P}_{ao}$ levels, whereas σ_H increased only at 5 and 10 cm H_2O. Both μ_H and σ_H demonstrated dependence on $\bar{P}_{ao}$ after ALI, with postinjury values at 5 cm H_2O significantly increased compared with 10, 15, and 20 cm H_2O. The σ_H was significantly increased compared with baseline at 5 and 10 cm H_2O.

Discussion

The heterogeneous nature of ALI is characterized by mechanically disparate lung regions, including collapsed

Table 2. Summary of Akaike Weights for Model Distributions with Lowest AIC_C Score

	$\bar{P}_{ao}$ = 5 cm H2O	$\bar{P}_{ao}$ = 10 cm H2O	$\bar{P}_{ao}$ = 15 cm H2O	$\bar{P}_{ao}$ = 20 cm H2O
Baseline	86.0 ± 15.4% (58.2–99.6%), n = 11	90.5 ± 16.0% (55.3–99.9%), n = 11	90.0 ± 18.1% (50.0–99.9%), n = 8	85.4 ± 20.4% (50.5–99.9%), n = 10
After injury	60.2 ± 0.09% (52.3–69.2%), n = 4	71.4 ± 21.3% (50.0–98.4%), n = 8	77.8 ± 26.2% (39.6–99.9%), n = 7	71.7 ± 23.9% (42.7–99.6%), n = 9

Data are expressed as mean ± SD of percent likelihood that the selected model generated the respiratory impedance (Z_{rs}) data at each condition and mean airway pressure ($\bar{P}_{ao}$). Parentheses denote the range of likelihoods at each condition and $\bar{P}_{ao}$, and n represents the number of dogs for which two or more model distributions converged to a unique solution using the nonlinear gradient search algorithm.

AIC_C = corrected Akaike Information Criterion.

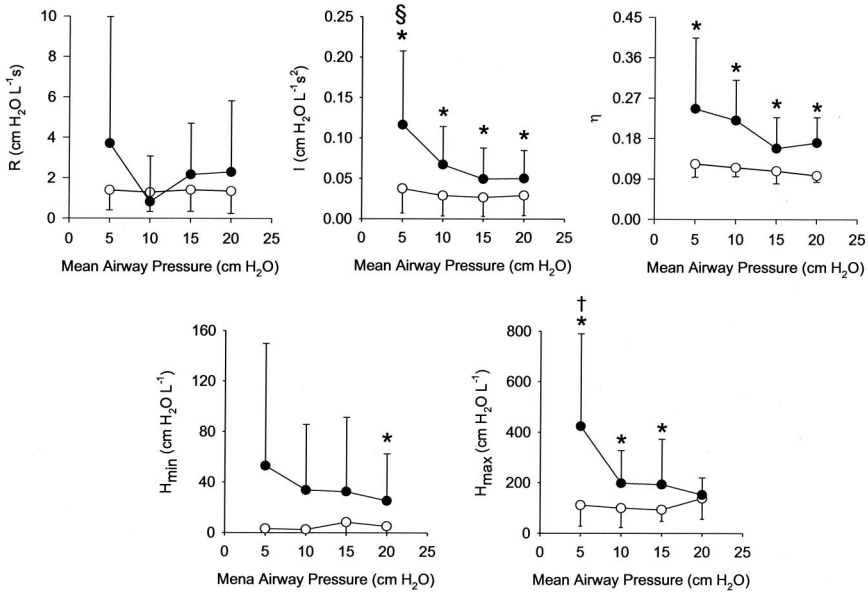

Fig. 7. Summary of model parameters *R*, *I*, η, H_{min}, and H_{max} *versus* mean airway pressure ($\bar{P}_{ao}$) for all 11 dogs. Data are shown at baseline (○) and after lung injury (●). Values are presented as mean ± SD. * Significantly higher from baseline data at same $\bar{P}_{ao}$ using two-tailed paired *t* test. † Significantly higher than corresponding data at 10, 15, and 20 cm H_2O at same condition using analysis of variance and least significant difference criterion. § Significantly higher than corresponding data at 15 and 20 cm H_2O at same condition using analysis of variance and least significant difference criterion.

nonventilated regions, injured but recruitable regions, normally ventilated regions, and overdistended regions prone to inflation injury. Recently, an "open-lung approach" to ventilation in these patients has been advocated, using PEEP to recruit collapsed lung units and improve oxygenation and low tidal volumes to minimize the risk of overdistention injury.[3] However, optimal PEEP and tidal volume for injured lungs are difficult to determine. Although PEEP may improve compliance in some regions of the lung by recruiting alveoli, it may simultaneously decrease compliance in other regions by overstretching units.

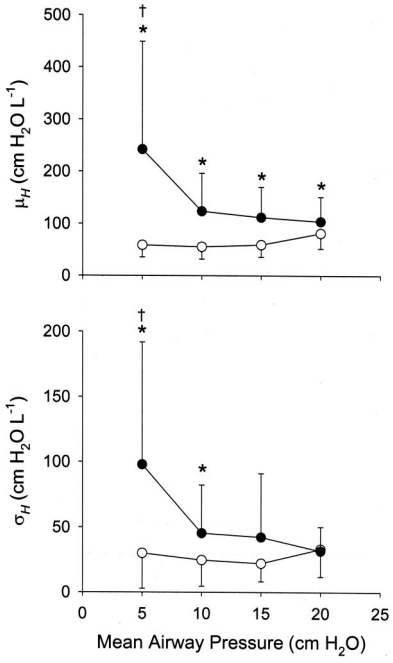

Fig. 8. Effective mean tissue elastance (μ_H) and heterogeneity index (σ_H) for all 11 dogs. Data are shown at baseline (○) and after lung injury (●). Values are presented as mean ± SD. * Significantly higher from baseline data at same mean airway pressure ($\bar{P}_{ao}$) using two-tailed paired *t* test. † Significantly higher from corresponding data at 10, 15, and 20 cm H_2O at same condition using analysis of variance and least significant difference criterion.

In the past, quasi-static pressure–volume curves were thought to provide insight into the "safe" ranges over which lung recruitment and overdistention injuries occur and therefore have been proposed for use in optimizing the mechanical stresses placed on the lungs during positive-pressure ventilation[30,31] and more recently during high-frequency ventilation.[32,33] However, as static measurements constructed under periods of zero flow, these curves provide no information regarding the dynamic regional mechanics in the lung or insight into the nature and distribution of lung injury during mechanical ventilation. Simple dynamic measure indices of lung mechanics, such as resistance and elastance measured at a single breathing frequency, can provide some insight into gross pathophysiology of the entire respiratory system but can be misleading if used to interpret regional mechanics of the lungs in the complex pathophysiology of ALI or to optimize ventilation strategy under varying conditions of frequency, tidal volume, or PEEP.[34–36] More recently, Ranieri *et al.* [37] characterized the concavity of the airway pressure–time curve during constant flow inflation with a power law expression to infer the balance between intratidal recruitment and overdistention occurring on a whole lung scale. Although this simple "stress index" may have some predictive value for the development of ventilator-associated lung injury, it does not quantify regional mechanical heterogeneity, which may be a more sensitive indicator. Multibreath inert gas washouts have also been used to detect the presence of heterogeneity and follow trends during the development of ALI,[38] but these approaches do not

directly quantify heterogeneity or changes in the mechanical properties of the respiratory tissues. Finally, other investigators have used high resolution computed tomography to assess heterogeneity in ALI,[39,40] although such a technique is not amenable to bedside implementation. Given the paucity of techniques available to assess heterogeneity in ALI, the ability to optimize the delicate balance of recruitment, oxygenation, and overdistention in this syndrome remains a challenge.

Heterogeneity and Respiratory Impedance

In 1956, Otis *et al.*[25] were the first to demonstrate how parallel time constant heterogeneity in the lung can cause frequency dependence in R_{rs} and E_{rs} . Since then, other groups have shown that the mechanical impedance spectrum of the lungs or total respiratory system can be a sensitive indicator of mechanical heterogeneity.[6,8,20,41,42] Using a computer-generated (but anatomically accurate) airway tree, Lutchen *et al.*[6,8,12,14] demonstrated that two distinct pathophysiologic mechanisms can be uniquely identified from Z_{rs}: (1) parallel time constant heterogeneity, which results in enhanced frequency dependence of R_{rs} and E_{rs} predominately below 2 Hz; and (2) random airway closure and derecruitment of lung units, which results in less lung tissue in communication with the airway opening and hence an increase in the levels of R_{rs} and E_{rs} throughout the entire bandwidth of interest. Both of these mechanisms can substantially increase R_{rs} and E_{rs} near breathing frequencies, exclusive of large increases in either overall airway resistance or actual tissue elasticity.[12]

Our Z_{rs} data are surprisingly similar to those data reported in many of these earlier modeling studies. At baseline, both R_{rs} and E_{rs} are dependent on frequency, which has been attributed primarily to the viscoelastic properties of the parenchymal tissues and chest wall in the healthy respiratory system,[11,29,34,43,44] although some baseline mechanical heterogeneity may also contribute to frequency dependence.[7,14,22,45] Under control conditions, we observed significant increases in E_{rs} and $|\bar{Z}_{rs}|$ with increasing $\bar{P}_{ao}$, which may result from overstretching and plastoelastic phenomena.[46] After lung injury, we observed significant increases in $|\bar{Z}_{rs}|$ and both the levels and frequency dependence of R_{rs} and E_{rs} at all values of $\bar{P}_{ao}$, indicating widespread mechanical heterogeneity and loss of alveolar units in communication with the airway opening as edema fluid fills air spaces. In contrast to baseline conditions, E_{rs} and $|\bar{Z}_{rs}|$ both decreased with increasing $\bar{P}_{ao}$ after ALI, consistent with the notion that moderate increases in $\bar{P}_{ao}$ are beneficial by reducing heterogeneity and recruiting lung units.

Model Analysis

To further quantify mechanical heterogeneity from our Z_{rs} data, we relied on the distributed modeling approach initially developed by Suki and coworkers[19,21] to describe the mechanical properties of the lungs during bronchoconstriction. More recently, this group proposed a similar analysis to describe the heterogeneity of tissue elastances in mouse model of emphysema, which predicts frequency dependence in both R_{rs} and E_{rs} not only by the mechanism of parallel heterogeneity, but also by viscoelasticity of the respiratory tissues.[20] They used only a hyperbolic distribution of tissue elastances to characterize Z_{rs}, whereas our data suggest that other tissue distribution functions may in fact be more appropriate to describe the dynamic behavior of the respiratory system after lung injury in dogs. In normal lungs, the AIC_C predicts that the linear distribution of tissue elastances was most appropriate for describing Z_{rs} in most dogs regardless of $\bar{P}_{ao}$. After lung injury, there was an increase in the number of dogs for which Z_{rs} was best characterized by a uniform distribution of tissue elastances. Nonetheless, most dogs were still best described by a linear distribution of elastances.

Although the model distribution with the lowest AIC_C score was most likely to have generated the data, it is important to understand that the AIC_C does not provide information regarding how well a particular distribution outperforms the other candidate distributions or the relative likelihood that this distribution generated the data. We determined this information using the technique of Akaike weights.[28] For the majority of dogs, the likelihood that the selected distribution generated the data were unequivocal (*i.e.*, $> 95\%$), although for a few dogs, the distinction between distributions was not as clear, particularly after lung injury (table 2).

Surprisingly, our R parameter demonstrated no significant dependence on $\bar{P}_{ao}$.[20,44,47] Although the value of R is composed of both airway resistance and Newtonian chest wall resistance, both may be influenced by thoracic volume to different extents.[24] This may mask any detectable relation between R and $\bar{P}_{ao}$. The I parameter, which in the healthy respiratory system primarily reflects the inertia of gas in the central airways, was significantly increased after ALI. This may result from a net increase in the oscillating mass of lung tissue due to the accumulation of edema fluid in the air spaces.

The progressive decrease in the average dynamic elastance parameter μ_H with increasing $\bar{P}_{ao}$ in injured animals is consistent with lung recruitment and previous reports of changes in the static lung elastance as a consequence of alveolar flooding and airway closure.[30,48] Therefore, it is unlikely that changes in μ_H reflect alterations in the actual elastic properties of the parenchymal tissues or chest wall. Baseline values of our heterogeneity index σ_H demonstrated a decreasing trend with $\bar{P}_{ao}$ up to 15 cm H_2O but increased slightly at 20 cm H_2O, although this did not achieve statistical significance. Although this is consistent with lung recruitment and decreases in mechanical heterogeneity, higher levels of $\bar{P}_{ao}$ may result in overdistention occurring in a somewhat heterogeneous manner. After lung injury, σ_H increased

significantly compared with baseline at 5 and 10 cm H_2O, implying an increase in mechanical heterogeneity. In addition, ANOVA demonstrated a significant dependence of σ_H on $\bar{P}_{ao}$ after ALI, with its highest value at 5 cm H_2O. Further increases in $\bar{P}_{ao}$ seem to reduce σ_H, also consistent with lung recruitment.

We observed significant increases in our hysteresivity parameter η after ALI. Hysteresivity has been proposed by Fredberg and Stamenovic[29] as an index to describe the hysteretic pressure–volume relation of the lung tissues and can be thought of as a ratio of energy dissipation to energy storage during cyclic changes in lung volume. It has long been held that η is relatively constant across lung volume, breathing frequency, and tidal volume.[29] However, these assumptions have been called into question in recent studies,[47,49] especially in animal models of ALI.[50,51] A key assumption of our modeling analysis is that η is constant throughout the respiratory tissues regardless of disease condition.[20,29] Our observed increases in η after ALI may reflect actual changes in the coupling of energy dissipation and storage in the respiratory tissues.[29] Hysteresivity is known to be influenced by several factors, including surface forces of the air–tissue interface, Coulomb friction between collagen and elastin fibers, and cross-bridge cycling in airway smooth muscle or other contractile elements in the lung parenchyma, any of which may be influenced by ALI. Moreover, there may be additional airway or tissue heterogeneity that is not appropriately described by our distribution functions, resulting in modeling error with an artifactually high estimate of η.[9,11,41]

Limitations

Despite the apparent utility of our approach to quantify mechanical heterogeneity in the respiratory system, these techniques rely on a few key assumptions that must be considered when using them to quantify regional mechanics. First, for mathematical convenience and simplicity, we evaluated only three simple tissue distribution functions to describe respiratory system heterogeneity as assessed at the airway opening. Although it seems that the Z_{rs} of most dogs is best described by a linear distribution of tissue elastances, we cannot be certain how accurately these functions describe actual tissue variability. Such information is probably more accurately obtained using functional computed tomography to quantify specific elastances.[39] Future studies may incorporate similar modeling approaches with imaging data to obtain more accurate tissue distribution functions for describing Z_{rs}. Therefore, although the current accuracy of our heterogeneity estimates may be somewhat biased because of modeling error, σ_H may still be a useful marker to assess the degree of heterogeneity in the lungs.

In addition, our modeling approach assumes that tissue heterogeneity is randomly distributed throughout the lungs and, as such, does not provide specific anatomic information on regional mechanics. Tissue heterogeneity in ALI may be distributed in a more deterministic manner, depending on the etiology of the injury, orientation in the gravitational field, local pulmonary blood flow, or proximity to the pleura or other organs. Whether such additional anatomical information would be useful in optimizing ventilatory parameters is unknown.

Finally, we recognize that our modeling analysis accounts only for tissue heterogeneity. Airway heterogeneity may also contribute to the enhanced frequency dependence in R_{rs} and E_{rs},[6,12,19,21,41] although the degree to which it does so in ALI is not clear. A previous study by Barnas *et al.*[44] using alveolar capsules in dogs demonstrated that increases in the frequency dependence of lung resistance and elastance after oleic acid–induced pulmonary edema were due primarily to changes in parenchymal tissue mechanics, implying that changes in airway resistance are not significant in the oleic acid model of lung injury. Similarly, our model analysis demonstrated no significant differences between preinjury and postinjury R. Therefore, we believe it is unlikely that airway heterogeneity contributed significantly to the frequency dependence we observed in R_{rs} and E_{rs} after ALI.

Summary

In summary, these data demonstrate that Z_{rs} can provide specific information about the mechanical heterogeneity of the lungs and the impact of $\bar{P}_{ao}$. After lung injury, both the level and frequency dependence of R_{rs} and E_{rs} increase compared with baseline, indicating the presence of widespread mechanical heterogeneity. These differences seem to be reduced by increases in $\bar{P}_{ao}$, consistent with the recruitment of lung units and minimization of the impact of heterogeneity on dynamic respiratory mechanics. Model analysis of Z_{rs} demonstrate that both effective tissue elastance and mechanical heterogeneity increase after ALI and decrease with increasing $\bar{P}_{ao}$. These noninvasive approaches may be useful in identifying optimal PEEP levels and tidal volume during conventional mechanical ventilation and possibly allow for the development of ventilation protocols to optimize regional lung mechanics in patients with ALI. Future research should be directed toward the development of more accurate tissue distribution functions to quantify the heterogeneity of injured lungs, which will be essential in the validation of this technique as a clinical diagnostic tool.

The authors thank H. Pierre Burman (Senior Animal Technician) and Kathleen K. Kibler (Laboratory Manager, Anesthesiology and Critical Care Medicine, Johns Hopkins University, Baltimore, Maryland) for technical assistance in this study.

References

1. Ware LB, Matthay MA: The acute respiratory distress syndrome. N Engl J Med 2000; 342:1334–49
2. Pelosi P, Cereda M, Foti G, Giacomini M, Pesenti A: Alterations of lung and chest wall mechanics in patients with acute lung injury: Effects of positive end-expiratory pressure. Am J Resp Crit Care Med 1995; 152:531–7
3. Amato MBP, Barbas CSV, Medeiros DM, Magaldi RB, Schettino GPP, Lorenzi-Filho G, Kairalla RA, Deheinzelin D, Munoz C, Oliveira R, Takagaki TY, Carvalho CRR: Effect of a protective-ventilation strategy on mortality in the acute respiratory distress syndrome. N Engl J Med 1998; 338:347–54
4. Gattinoni L, Vagginelli F, Chiumello D, Taccone P, Carlesso E: Physiologic rationale for ventilator setting in acute lung injury/acute respiratory distress syndrome patients. Crit Care Med 2003; 31:S300–4
5. Lutchen KR, Suki B: Understanding pulmonary mechanics using the forced oscillations technique, Bioengineering Approaches to Pulmonary Physiology and Medicine. Edited by Khoo MCK . New York, Plenum Press, 1996, pp 227–53
6. Lutchen KR, Greenstein JL, Suki B: How inhomogeneities and airway walls affect frequency dependence and separation of airway and tissue properties. J Appl Physiol 1996; 80:1696–707
7. Lutchen KR, Hantos Z, Jackson AC: Importance of low-frequency impedance data for reliably quantifying parallel inhomogeneities of respiratory mechanics. IEEE Trans Biomed Eng 1988; 35:472–81
8. Lutchen KR, Gillis H: Relationship between heterogeneous changes in airway morphometry and lung resistance and elastance. J Appl Physiol 1997; 83:1192–201
9. Kaczka DW, Ingenito EP, Israel E, Lutchen KR: Airway and lung tissue mechanics in asthma: Effects of albuterol. Am J Resp Crit Care Med 1999; 159:169–78
10. Kaczka DW, Ingenito EP, Body SC, Duffy SE, Mentzer SJ, DeCamp MM, Lutchen KR: Inspiratory lung impedance in COPD: Effects of PEEP and immediate impact of lung volume reduction surgery. J Appl Physiol 2001; 90:1833–41
11. Kaczka DW, Ingenito EP, Suki B, Lutchen KR: Partitioning airway and lung tissue resistances in humans: Effects of bronchoconstriction. J Appl Physiol 1997; 82:1531–41
12. Lutchen KR, Jensen A, Atileh H, Kaczka DW, Israel E, Suki B, Ingenito EP: Airway constriction pattern is a central component of asthma severity: The role of deep inspirations. Am J Resp Crit Care Med 2001; 164:207–15
13. Gillis HL, Lutchen KR: Airway remodeling in asthma amplifies heterogeneities in smooth muscle shortening causing hyperresponsiveness. J Appl Physiol 1999; 86:2001–12
14. Gillis HL, Lutchen KR: How heterogenous bronchoconstriction affects ventilation distribution in human lungs: A morphometric model. Ann Biomed Eng 1999; 27:14–22
15. Navalesi P, Hernandez P, Laporta D, Landry JS, Maltais F, Navajas D, Gottfried SB: Influence of site of tracheal pressure measurement on in situ estimation of endotracheal tube resistance. J Appl Physiol 1994; 77:2899–906
16. Kaczka DW, Lutchen KR: Servo-controlled pneumatic pressure oscillator for respiratory impedance measurements and high frequency ventilation. Ann Biomed Eng 2004; 32:596–608
17. Suki B, Lutchen KR: Pseudorandom signals to estimate apparent transfer and coherence functions of nonlinear systems: applications to respiratory mechanics. IEEE Trans Biomed Eng 1992; 39:1142–51
18. Daroczy B, Hantos Z: An improved forced oscillatory estimation of respiratory impedance. Int J Biomed Comput 1982; 13:221–35
19. Suki B, Yuan H, Zhang Q, Lutchen KR: Partitioning of lung tissue response and inhomogeneous airway constriction at the airway opening. J Appl Physiol 1997; 82:1349–59
20. Ito S, Ingenito EP, Arold SP, Parameswaran H, Tgavalekos NT, Lutchen KR, Suki B: Tissue heterogeneity in the mouse lung: Effects of elastase treatment. J Appl Physiol 2004; 97:204–12
21. Yuan H, Suki B, Lutchen KR: Sensitivity analysis for evaluating nonlinear models of lung mechanics. Ann Biomed Eng 1998; 26:230–41
22. Sakai H, Ingenito EP, Mora R, Abbay S, Cavalcante FSA, Lutchen KR, Suki B: Hysteresivity of the lung and tissue strip in the normal rat: Effects of heterogeneities. J Appl Physiol 2001; 91:737–47
23. Hantos Z, Daroczy B, Csendes T, Suki B, Nagy S: Modeling of low-frequency pulmonary impedance in dogs. J Appl Physiol 1990; 68:849–60
24. Black LD, Dellaca R, Jung K, Atileh H, Israel E, Ingenito EP, Lutchen KR: Tracking variations in airway caliber by using total respiratory vs. airway resistance in healthy and asthmatic subjects. J Appl Physiol 2003; 95:511–8
25. Otis AB, McKerrow CB, Bartlett RA, Mead J, McIlroy MB, Selverstone NJ, Radford Jr EP: Mechanical factors in the distribution of pulmonary ventilation. J Appl Physiol 1956; 8:427–43
26. Akaike H: A new look at the statistical model identification. IEEE Trans Automat Contr 1974; 19:716–23
27. Motulsky H, Christopoulos A: Fitting Models to Biological Data using Linear and Nonlinear Regression: A Practical Guide to Curve Fitting. New York, Oxford University Press, 2004, pp 143–8
28. Wagenmakers E-J, Farrell S: AIC model selection using Akaike weights. Psychon Bull Rev 2004; 11:192–6
29. Fredberg JJ, Stamenovic D: On the imperfect elasticity of lung tissue. J Appl Physiol 1989; 67:2048–419
30. Grossman RF, Jones JG, Murray JF: Effects of oleic acid-induced pulmonary edema in lung mechanics. J Appl Physiol 1980; 48:1045–51
31. Venegas JG, Harris RS, Simon BA: A comprehensive equation for pulmonary pressure-volume curve. J Appl Physiol 1998; 84:389–95
32. Luecke T, Meinhardt JP, Herman P, Weisser G, Pelosi P, Quintel M: Setting mean airway pressure during high-frequency ventilation according to the static pressure–volume curve in surfactant-deficient lung injury: A computed tomographic study. ANESTHESIOLOGY 2003; 99:1313–22
33. Goddon S, Fujino Y, Hromi JM, Kacmarek RM: Optimal mean airway pressure during high-frequency oscillation predicted by the pressure–volume curve. ANESTHESIOLOGY 2001; 94:862–9
34. Kaczka DW, Barnas GM, Suki B, Lutchen KR: Assessment of time-domain analyses for estimation of low-frequency respiratory mechanical properties and impedance spectra. Ann Biomed Eng 1995; 23:135–51
35. Barnas GM, Harinath P, Green MD, Suki B, Kaczka DW, Lutchen KR: Influence of waveform and analysis technique on lung and chest wall properties. Respir Physiol 1994; 96:331–44
36. Lutchen KR, Kaczka DW, Suki B, Barnas G, Cevenini G, Barbini P: Low-frequency respiratory mechanics using ventilator-driven forced oscillations. J Appl Physiol 1993; 75:2549–60
37. Ranieri VM, Zhang H, Mascia L, Aubin M, Lin C-Y, Mullen B, Grasso S, Binnie M, Volgyesi GA, Slutsky AS: Pressure–time curve predicts minimally injurious ventilatory strategy in an isolated rat lung model. ANESTHESIOLOGY 2000; 93:1320–8
38. Tsang JYC, Emery MJ, Hlastala MP: Ventilation inhomogeneity in oleic acid-induced pulmonary edema. J Appl Physiol 1997; 82:1040–5
39. Simon BA: Non-invasive imaging of regional lung function using x-ray computed tomography. J Clin Monit 2000; 16:433–42
40. Gattinoni L, Pelosi P, Crotti S, Valenza F: Effects of positive end-expiratory pressure on regional distribution of tidal volume and recruitment in adult respiratory distress syndrome. Am J Resp Crit Care Med 1995; 151:1807–14
41. Lutchen KR, Hantos Z, Petak F, Adamicza A, Suki B: Airway inhomogeneities contribute to apparent lung tissue mechanics during constriction. J Appl Physiol 1996; 80:1841–9
42. Hantos Z, Daroczy B, Suki B, Nagy S, Fredberg JJ: Input impedance and peripheral inhomogeneity of dog lungs. J Appl Physiol 1992; 72:168–78
43. Barnas GM, Stamenovic D, Lutchen KR: Lung and chest wall impedances in the dog in normal range of breathing: Effects of pulmonary edema. J Appl Physiol 1992; 73:1040–6
44. Barnas GM, Sprung J, Kahn R, Delaney PA, Agarwal M: Lung tissue and airway impedance during pulmonary edema in the normal range of breathing. J Appl Physiol 1995; 78:1889–97
45. Warner DO: Alveolar pressure inhomogeneity during low-frequency oscillation of excised canine lobes. J Appl Physiol 1990; 69:155–61
46. Stamenovic D, Lutchen KR, Barnas GM: Alternative model of respiratory tissue viscoplasticity. J Appl Physiol 1993; 75:1062–9
47. Hantos Z, Collins RA, Turner DJ, Janosi TZ, Sly PD: Tracking of airway and tissue mechanics during TLC maneuvers in mice. J Appl Physiol 2003; 95:1695–705
48. Slutsky AS, Scharf SM, Brown R, Ingram RH: The effect of oleic acid-induced pulmonary edema on pulmonary and chest wall mechanics in dogs. Am Rev Respir Dis 1980; 121:91–6
49. Sly PD, Collins RA, Thamrin C, Turner DJ, Hantos Z: Volume dependence of airway and tissue impedances in mice. J Appl Physiol 2003; 94:1460–6
50. Allen G, Lundblad LKA, Parsons P, Bates JHT: Transient mechanical benefits of a deep inflation in the injured mouse lung. J Appl Physiol 2002; 93: 1709–15
51. Allen G, Bates JHT: Dynamic mechanical consequences of deep inflation in mice depend on type and degree of lung injury. J Appl Physiol 2004; 96:293–300

Appendix

The model-predicted impedance ($\hat{Z}_{rs}$) of the network of figure 1 can be defined as the reciprocal of the sum of admittances of each branch:

$$\hat{Z}_{rs}(\omega)=\left(\sum_{n=1}^{N}\frac{1}{R+j\omega I+\frac{(\eta-j)H_n}{\omega^{\alpha}}}\right)^{-1} \tag{1}$$

with

$$\alpha=\frac{2}{\pi}\tan^{-1}\left(\frac{1}{\eta}\right) \tag{2}$$

and where j is the unit imaginary number, ω is the angular frequency, and N is the number of branches in the network. Alternatively, if we assume that the variation in tissue elastance between branches varies in a probabilistic manner, we can approximate $\hat{Z}_{rs}$ as

$$\hat{Z}_{rs}(\omega)=\left(\sum_{m=1}^{M}\frac{P_{\Delta H}(H_m)}{R+j\omega I+\frac{(\eta-j)H_m}{\omega^{\alpha}}}\right)^{-1} \tag{3}$$

where $P_{\Delta H}$ represents a histogram function of bin width ΔH, H_m denotes the center value of elastances stored in bin m, and M is the total number of bins in the distribution. In the limit as the number of branches tends toward infinity and ΔH approaches zero, we obtain an expression for $\hat{Z}_{rs}$ that depends on a continuous probability density function $P(H)$ integrated over the upper and lower bounds H_{min} and H_{max}:

$$\hat{Z}_{rs}(\omega)=\left(\int_{H_{min}}^{H_{max}}\frac{P(H)}{R+j\omega I+\frac{(\eta-j)H}{\omega^{\alpha}}}dH\right)^{-1} \tag{4}$$

Regardless of the form of $P(H)$, we can define an effective mean tissue elastance, μ_H, which provides a rough estimate of the overall elastance of the respiratory tissues:

$$\mu_H=\int_{H_{min}}^{H_{max}}HP(H)dH \tag{5}$$

To quantify the heterogeneity of the respiratory tissues, we relied on the SD σ_H of $P(H)$:

$$\sigma_H=\sqrt{\int_{H_{min}}^{H_{max}}(H-\mu_H)^2P(H)dH} \tag{6}$$

To obtain simple, closed-form expressions for equation 4, we defined a probability density function $P(H)$ *a priori* to be of the form

$$P(H)=\begin{cases}\frac{L}{H^{\lambda}}, & H_{max}\geq H\geq H_{min}\\ 0 & otherwise\end{cases} \tag{7}$$

where L is a constant which depends on H_{min} and H_{max} as well as the function $P(H)$. We assume $\lambda = -1, 0, 1$, which define models corresponding to linear, uniform, and hyperbolic distributions of tissue elastances, respectively (fig. 3). An expression for L can be obtained by assuming that the area under the probability density function $P(H)$ is equal to 1:

$$L=\frac{1}{\int_{H_{min}}^{H_{max}}\frac{dH}{H^{\lambda}}} \tag{8}$$

Thus, using equation 7 with $\lambda = -1$ to solve for equations 4, 5, and 6, we obtain for the linear distribution,

$$\hat{Z}_{rs}(\omega)=\frac{\left(H_{max}^2-H_{min}^2\right)(\eta-j)}{2\omega^{\alpha}\left[(\eta-j)(H_{max}-H_{min})-\omega^{\alpha}(R+j\omega I)\ln\left(\frac{R+j\omega I+\frac{(\eta-j)H_{max}}{\omega^{\alpha}}}{R+j\omega I+\frac{(\eta-j)H_{min}}{\omega^{\alpha}}}\right)\right]} \tag{9}$$

$$\mu_H=\frac{2}{3}\left(\frac{H_{max}^3-H_{min}^3}{H_{max}^2-H_{min}^2}\right) \tag{10}$$

$$\sigma_H=\sqrt{\frac{\frac{1}{2}\left(H_{max}^4-H_{min}^4\right)-\frac{4}{3}\mu_H\left(H_{max}^3-H_{min}^3\right)+\mu_H\left(H_{max}^2-H_{min}^2\right)}{H_{max}^2-H_{min}^2}} \tag{11}$$

and with $\lambda = 0$ for the uniform distribution

$$\hat{Z}_{rs}(\omega)=\frac{(H_{max}-H_{min})(\eta-j)}{\omega^{\alpha}\left[\ln\left(\frac{R+j\omega I+\frac{(\eta-j)H_{max}}{\omega^{\alpha}}}{R+j\omega I+\frac{(\eta-j)H_{min}}{\omega^{\alpha}}}\right)\right]} \tag{12}$$

$$\mu_H=\frac{1}{2}\left(\frac{H_{max}^2-H_{min}^2}{H_{max}-H_{min}}\right) \tag{13}$$

$$\sigma_H=\sqrt{\frac{\frac{1}{3}\left(H_{max}^3-H_{min}^3\right)-\mu_H\left(H_{max}^2-H_{min}^2\right)+\mu_H^2\left(H_{max}-H_{min}\right)}{H_{max}-H_{min}}} \tag{14}$$

and finally with $\lambda = 1$ for the hyperbolic distribution,

$$\hat{Z}_{rs}(\omega)=\frac{\left(\ln\left(\frac{H_{max}}{H_{min}}\right)\right)(R+j\omega I)}{\left[\ln\left(\frac{H_{max}}{H_{min}}\right)-\ln\left(\frac{R+j\omega I+\frac{(\eta-j)H_{max}}{\omega^{\alpha}}}{R+j\omega I+\frac{(\eta-j)H_{min}}{\omega^{\alpha}}}\right)\right]} \tag{15}$$

$$\mu_H = \frac{H_{max} - H_{min}}{\ln\left(\frac{H_{max}}{H_{min}}\right)} \quad (16)$$

$$\sigma_H = \sqrt{\frac{\frac{1}{2}\left(H_{max}^2 - H_{min}^2\right) - 4\mu_H\left(H_{max} - H_{min}\right) + \mu_H \ln\left(\frac{H_{max}}{H_{min}}\right)}{\ln\left(\frac{H_{max}}{H_{min}}\right)}} \quad (17)$$

Note that for equations 9, 12, and 15, we define the natural logarithm of any arbitrary complex number $z = x + jy$ as

$$\ln(z) = \ln|z| + j\arg(z) = \ln\left(\sqrt{x^2 + y^2}\right) + j\tan^{-1}\left(\frac{y}{x}\right) \quad (18)$$